We 14 15

Two Seismic Interference Attenuation Methods Based on Automatic Detection of Seismic Interference Moveout

S. Jansen* (University of Oslo), T. Elboth (CGG) & C. Sanchis (CGG)

SUMMARY

The need for efficient seismic interference (SI) attenuation solutions is essential to reduce time-sharing that is very costly. We present two SI attenuation methods, both based on the automatic vector field estimation of the SI local moveout. The first method proposes an automatic determination of tau-p mute parameters, while the second one uses line integral convolution and the estimated vector field to separate SI from reflection hyperbolas. Because of the automatic detection of SI attributes, they require little user interaction and the processing time is short. Both methods are tested on real shot gathers and successfully attenuate the SI while preserving the reflections.

Introduction

A frequently encountered problem in seismic data is the presence of various types of coherent noise and in particular, marine seismic interference (SI). SI is encountered when several seismic vessels operate simultaneously in close proximity. If the amplitude and/or moveout of the SI exceed certain limits, then the operating vessels normally have to commence time-sharing. Unfortunately, this is costly and can also lead to significant delays in survey completion. Operating vessels have been known to commence time-sharing at distances up to 100 km. However, as a rough guideline, SI are often seen as problematic when vessels are closer than 40 km, which is often the case in busy summer seasons offshore Northern Europe and in the Gulf of Mexico.

Generally, SI and coherent noise removal algorithms can be classified into two groups. The first group is based on the realization that coherent energy in the shot domain often appears as random noise in other domains (Larner et al. 1983). Random noise attenuation tools like *f-x* prediction filtering (Canales 1984) or thresholding methods (Elboth et al. 2010) are then applied to the data, before it is sorted back to the shot domain. This SI attenuation approach has been used by Akbulut et al. (1984) and more recently by Gulunay (2008). However, in the case where shot-point intervals of interfering vessels are synchronized, SI appears at the same arrival time in consecutive shot gathers. Therefore, SI cannot be randomized when sorted to other domains and the whole approach breaks down. Another limitation concerns methods that involve amplitude thresholding. They require the SI amplitudes to be larger than the reflections amplitudes, which is not always the case.

The second group of SI removal tools is based on noise modelling and subtraction. An early example is Kirlin and Done (1990) that uses singular value decomposition to identify coherent events in the data and then subtract them. Finally, more recent approaches estimate the source position and/or firing times of the SI. The SI are then modelled and subtracted like in Brittan et al. (2008). The success of these methods strongly depends on their ability to build up an accurate model of the SI. This article presents a method for an automatic estimation of SI moveout, which is then used as an initial step in two techniques. The first technique consists of the automatic generation of a tau-*p* mute, while the second technique uses the line integral convolution method and an estimate of vector fields to separate SI from reflection hyperbolas.

SI moveout estimation

In a commercial setting where a processor has to go through gigabytes of data, the user interaction needs to be minimized. We present here a method that works on individual shot gathers and estimates the SI moveout without user interaction. This step will be used further by both techniques presented later.

We start by dividing the shot gather into J space windows where each window contains all the samples and the same number of traces. We scan each space window by using a small sliding window in time and space. In each sliding window, two neighbor traces are cross-correlated to obtain a vector $\vec{\mathbf{v}}_0 = (v_x \; v_t)^T$ that represents the local moveout in the data. The trace spacing v_x is always equal to 1 sample while v_t is the time delay in ms estimated by cross-correlation. For most windows, $\vec{\mathbf{v}}_0$ gives the local moveout of the reflection hyperbolas. However, if SI is present, $\vec{\mathbf{v}}_0$ may also represent the moveout of the SI. A total of K vectors $\vec{\mathbf{v}}_0$ are then estimated for each space window, as shown in Fig.1.

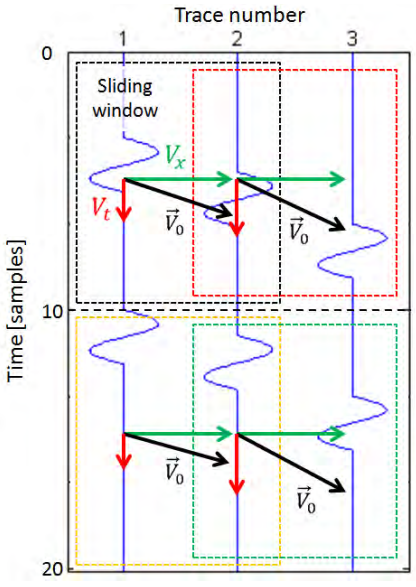

Figure 1 *Estimation of moveout vectors* $\vec{\mathbf{v}}_0$ *in each sliding window.*

The challenge now is to identify from the K vectors $\vec{\mathbf{v}}_0$ two different vector fields. One should indicate the moveout of the SI while the other should indicate the

moveout of the reflection hyperbolas. The reflections moveout vector field can be estimated by using knowledge of survey geometry and picked subsurface velocities. The moveout of the SI vector field, however, has to be identified.

SI usually arrives fairly linear through a shot gather compared to the reflection hyperbolas. Using this observation, we look at the distribution of the K moveout components v_t of vectors $\vec{\mathbf{v}}_0$ for each space window. Our assumption is that the vectors indicative of SI, coming from a significant distance, have a rather constant moveout in space and time while vectors indicative of reflection hyperbolas have more variations. In particular, v_t is smaller at near offset and increases with offset. Therefore, we expect the SI moveout to be the one with minimum relative standard deviation. For each moveout value of the distribution, $v_{t,i}$, the standard deviation $\sigma_{v,i}$ of the number of occurrences $n_{i,j}$ for $j=1,\ldots,J$, is calculated over the J representations available. The relative standard deviation is then the normalized standard deviation given by $\sigma_i = \frac{\sigma_{v,i}}{\max_j(n_{i,j})} \times 100$. Let us consider a real data example shown in Fig.3a with a single interfering vessel. This shot gather has been divided into $J=8$ space windows, containing 81 traces each. The distribution of v_t components for each space window is shown in Fig.2 (left), while Fig.2 (right) shows the relative standard deviation σ_i for each moveout value. The minimum σ_i is achieved at moveout $\hat{p} \equiv \arg\min_{v_{t,i}} \sigma_i \approx 1800$ ms. To validate this estimate, we transform this dataset to the tau-p domain and locate the moveout at approximately 1850 ms (Fig. 3c). This value is close to our SI moveout estimate $\hat{p}$ which is considered to be sufficiently accurate. Finally, we obtain an SI vector field in the shot gather $\mathbf{V}_0^{\mathbf{SI}}$ by keeping only the vectors whose estimated moveout is within $\hat{p} \mp \Delta p$ interval. In Fig.3c, $\Delta p = 300$ ms. The 2nd method requires a dense representation of vector field. Missing vectors are then interpolated and averaged over the existing ones to obtain one vector per sample location. We denote this dense SI vector field by $\mathbf{V}^{\mathbf{SI}}$.

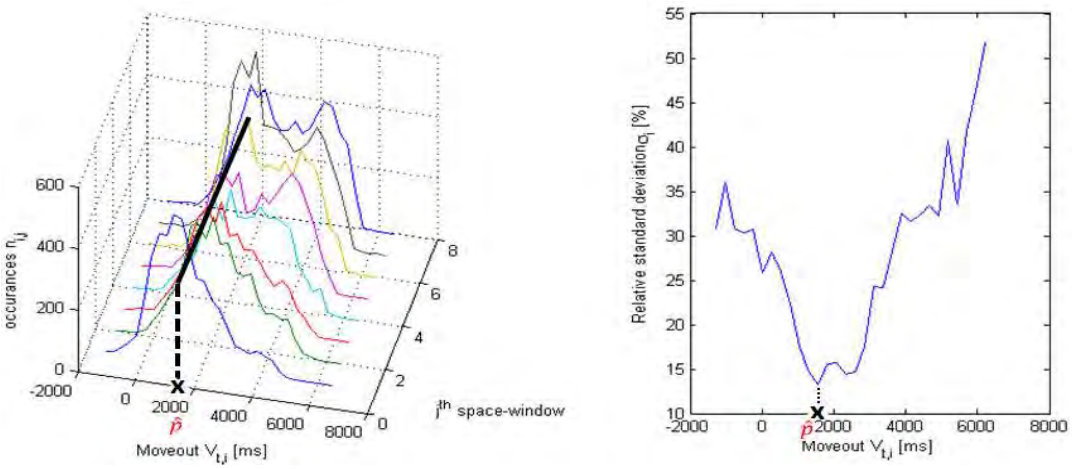

Figure 2 *(Left) Distribution of the moveout component v_t for $J=8$ equally sized windows. (Right) Relative standard deviation σ_i for each moveout value.*

Method 1: Automatic tau-*p* mute

Our first SI removal method consists of the generation of a tau-p mute using the SI moveout estimate $\hat{p}$. However, to refine the tau-p mute, we also estimate the central arrival time of the SI in the shot domain $\hat{\tau}$, thereby providing us with $\hat{\tau}$ in tau-p domain. To do so, for each sample of the first trace $(t'\ 1)^T$, we calculate the total distance (in samples) to all the vectors $(t_i\ \ x_i)^T$ of SI vector field $\mathbf{V}_0^{\mathbf{SI}}$: $d_{tot}(t') = \sum_i d_i$ where $d_i = \sqrt{(x_i - 1)^2 + (t_i - t')^2}$. Thereafter, an estimate of $\hat{\tau}$ is obtained at

minimum distance $\hat{\tau} \equiv \arg\min_{t'} d_{tot}$. The determination of $\hat{\tau}$ for our real dataset is shown in Fig. 3b. Thus, the estimation of $\hat{\tau}$ and $\hat{p}$ defines a fairly accurate tau-*p* mute shown in Fig. 3c (green window). Since a forward-inverse tau-*p* transform is not considered as signal preserving, we choose to mute out everything but the SI in tau-*p* domain and then perform an inverse tau-*p* transform. Finally, we adaptively subtract the SI from the original shot gather, providing an SI attenuated shot gather (Fig. 3d). The difference plot in Fig. 3e shows a good preservation of reflection data.

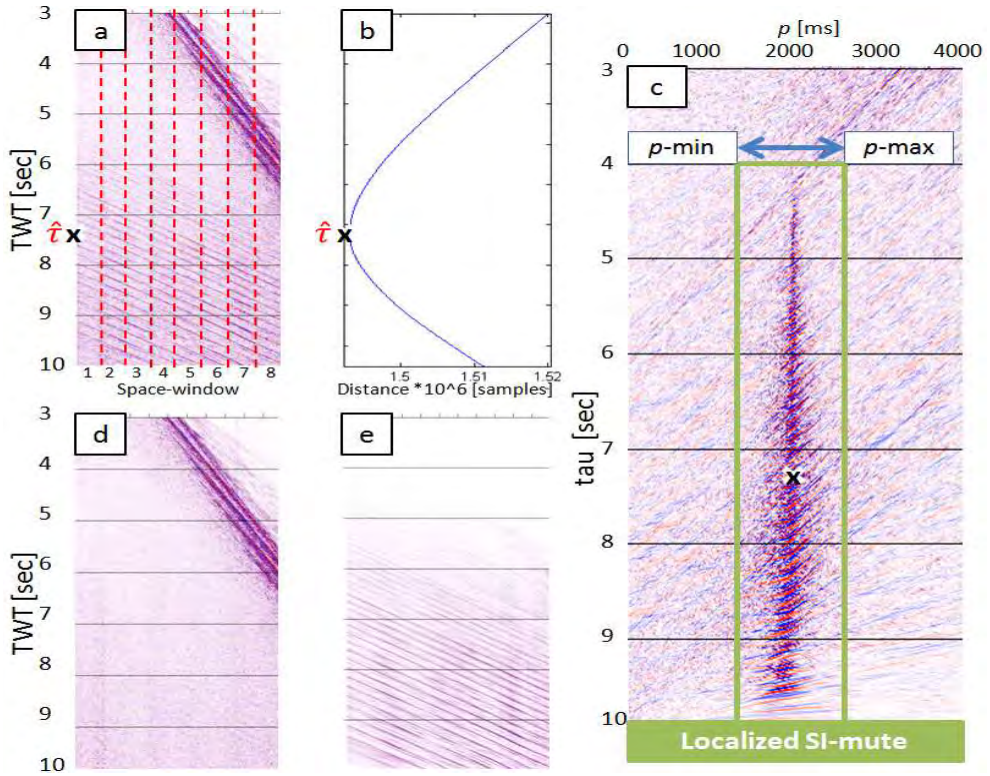

Figure 3 *a) A shot gather contaminated by SI, (b) the corresponding distance-plot, (c) tau-p representation and the localized SI mute, (d) shot gather after SI attenuation and (e) difference plot.*

Method 2: Line integral convolution

The second method uses a method referred to as line integral convolution (Cabral and Leedom 1993). The line integral convolution (LIC) is an imaging technique that uses texture advection to densely visualize vector fields and render images with a large amount of details. Compared with simpler integration-like techniques, where one follows the flow vector at each point to produce a line, it has the advantage of producing a whole image at every step. We have adapted the LIC technique for SI removal, taking advantage of the fact that SI can be expected to locally be rather coherent. For every sample of the input gather *(t , x)*, a local streamline that starts at this center sample is calculated in the forward and backward directions for *2L+1* samples, following the input vector field $\mathbf{V}^{\mathbf{SI}}$. The output value in *(t , x)* is then the median value of all the amplitudes along this streamline. Since SI is assumed to be coherent along the line integral, it adds up constructively. Conversely, the reflections hyperbolas are not coherent over the same line integral and in most cases just stack out. Here, LIC filters the input shot gather along local streamlines defined by $\mathbf{V}^{\mathbf{SI}}$ to generate an estimate of the SI with large amount of details. This SI estimate is then subtracted from the input shot gather to produce a SI attenuated gather.

Figure 4 shows two real shot gathers contaminated by SI from a single interfering vessel: one with SI from ahead and one with SI from astern (top and bottom, left). Both are processed with method 2 for

L=30 samples. Output gathers (middle) are fairly clean with SI successfully attenuated and the difference plots (right) show that reflection hyperbolas are well preserved.

Discussion and conclusion

We presented two efficient SI removal methods based on automatic SI moveout estimation. Both are fully data driven and only need one shot gather to be applied. The processing time is short and thereby, the methods have the potential to be applied in real-time while a seismic survey is conducted. As arrival time and direction of SI may change from shot to shot gathers, the automatic detection of attributes automatically generates accurate mutes with little interaction from the processor.

References

Akbulut, K., Saeland, O-K., Farmer, P., and Curtis, T. [1984] Suppression of seismic interference noise on Gulf of Mexico data. *SEG*, Expanded Abstracts, 527-529.
Brittan, J., Pidsley, L., Cavalin, D., Ryder, A. and Turner, G. [2008] Optimizing the removal of seismic interference noise. *The Leading Edge*, **27**, 166-175.
Cabral, B. and Leedom, L. C. [1993] Imaging Vector Fields Using Line Integral Convolution. *Proceedings of ACM SIGGRAPH 1993*, 263-272.
Canales, L. [1984] Random noise reduction. *SEG*, Expanded Abstracts, 525-527.
Elboth, T., Presterud, I. and Hermansen, D. [2010] Time-frequency seismic data de-noising. *Geophysical Prospecting*, **58**, No 3, 441–453.
Gulunay, N. [2008] Two different algorithms for seismic interference noise attenuation. *The Leading Edge*, **27**, 176-181.
Kirlin, R.L. and Done, W.J. [1990] Suppression of coherent noise in seismic data. US patent 4910716.
Larner, K., Chambers, R., Yang, M., Lynn, W., and Wai, W. [1983] Coherent noise in marine seismic data. *Geophysics*, **48**, 854-886.

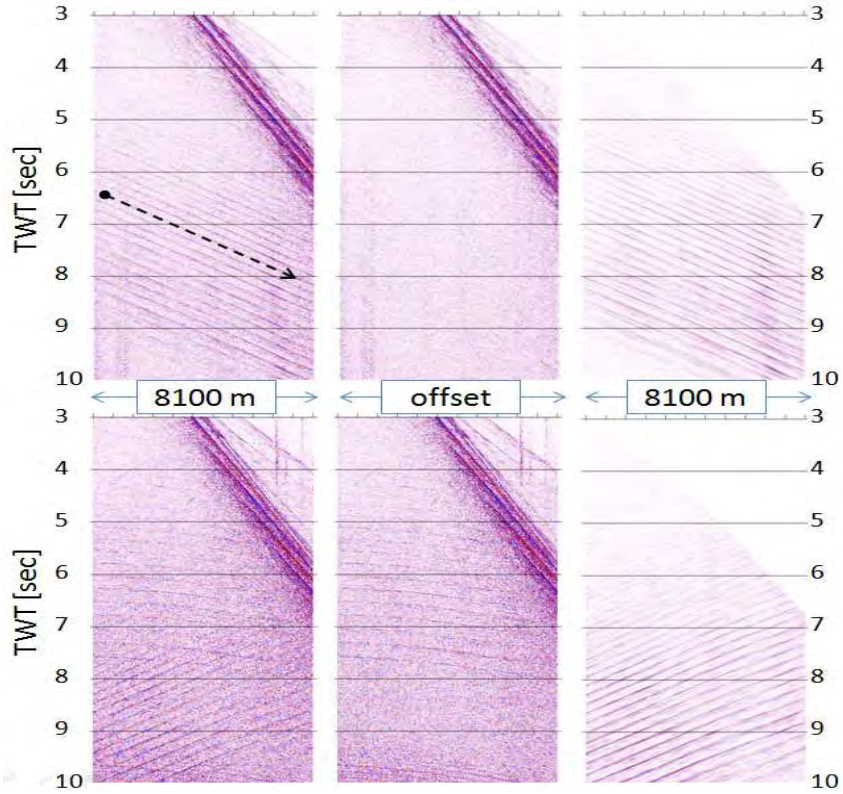

Figure 4 *Two shot gathers with SI from ahead (top left) and from astern (bottom left). Shot gathers after processing (middle) and difference plots (right). A streamline example is shown in top left.*